GeoHazards

MDPI

Article

The Northern Giona Fault Zone, a Major Active Structure Through Central Greece

Leonidas Gouliotis [1,*] and Dimitrios Papanikolaou [2]

[1] Energean, 15125 Athens, Greece
[2] Department of Geology and Geoenvironment, National & Kapodistrian University of Athens, 15771 Athens, Greece; dpapan@geol.uoa.gr
* Correspondence: lgouliotis@energean.com

Abstract: The steep northern slopes of Giona Mt in central continental Greece are the result of an E-W normal fault dipping 35–45° to the north, extending from the Mornos River in the west to the village of Gravia in the east. This fault creates a significant elevation difference of approximately 1500 m between the northern Giona footwall and the southern Iti hanging wall. The footwall comprises imbricated Mesozoic carbonates of the Parnassos unit, which exhibit large-scale drag folding near and parallel to the fault. The hanging wall comprises deformed sedimentary rocks of the Beotian unit and tectonic klippen of the Eastern Greece unit, forming a southward-tilted neotectonic block with subsidence near the Northern Giona Fault and uplift near the Ypati fault to the north. These two E-W faults represent younger structures disrupting the older NNW-trending tectonic framework. Fault scarps are observed all along the 14 km length of the Northern Giona fault accompanied by cataclastic zones, separating the carbonate formations of the Parnassos Unit from thick scree, slide blocks, boulders and olistholites. Inversion of fault-slip data has shown a mean slip vector of 45°, N004°E, which aligns with the current regional extensional deformation of the area, as confirmed by focal mechanism solutions. Based on the general asymmetry of the alpine units in the hanging wall, we interpret a listric fault geometry at depth using slip-line analysis and we forward modelled a disrupted fault-propagation fold using kinematic trishear algorithms, estimating a total displacement of 6500 m and a throw of approximately 2000 m. Seismic activity in the area of the Northern Giona Fault includes a magnitude 6.1 earthquake in 1852, which caused casualties, rockfalls and extensive damage, as well as a magnitude 5.1 event in 1983. The expected seismic magnitude is deterministically estimated between 6.2 and 6.7, depending on the potential westward continuation of the Northern Giona Fault beyond the Mornos River to the Northern Vardoussia saddle. The seismic hazard zone includes several villages located near the fault, particularly on the hanging wall, where intense landslide activity during seismic events could result in severe damage to regional infrastructure. The neotectonic development of the Northern Giona Fault highlights the importance of extending seismotectonic research into the mountainous regions of central Greece within the alpine formations, beyond the post-orogenic sedimentary basins.

Keywords: active tectonics; central Greece; forward modelling; Giona Mt; Iti Mt

Citation: Gouliotis, L.; Papanikolaou, D. The Northern Giona Fault Zone, a Major Active Structure Through Central Greece. *GeoHazards* **2024**, *5*, 1370–1388. https://doi.org/10.3390/geohazards5040065

Academic Editor: Dickson Cunningham

Received: 14 September 2024
Revised: 3 December 2024
Accepted: 12 December 2024
Published: 18 December 2024

1. Introduction

The mountainous region of eastern central Greece extends between two east–west transverse tectonic zones; in the north, the Sperchios Valley, which is drained by the Sperchios River flowing eastward to the Maliakos Gulf, and in the south, the Corinth Gulf. This high elevated area features four mountain ranges exceeding 2100 m in altitude. Giona Mt (2507 m) is the highest mountain in the region and the highest mountain of southern Greece. It is separated from Parnassos Mt (2455 m) to the east by the Amfissa valley and from Vardoussia Mt (2413 m) to the west by the Mornos River (Figure 1).

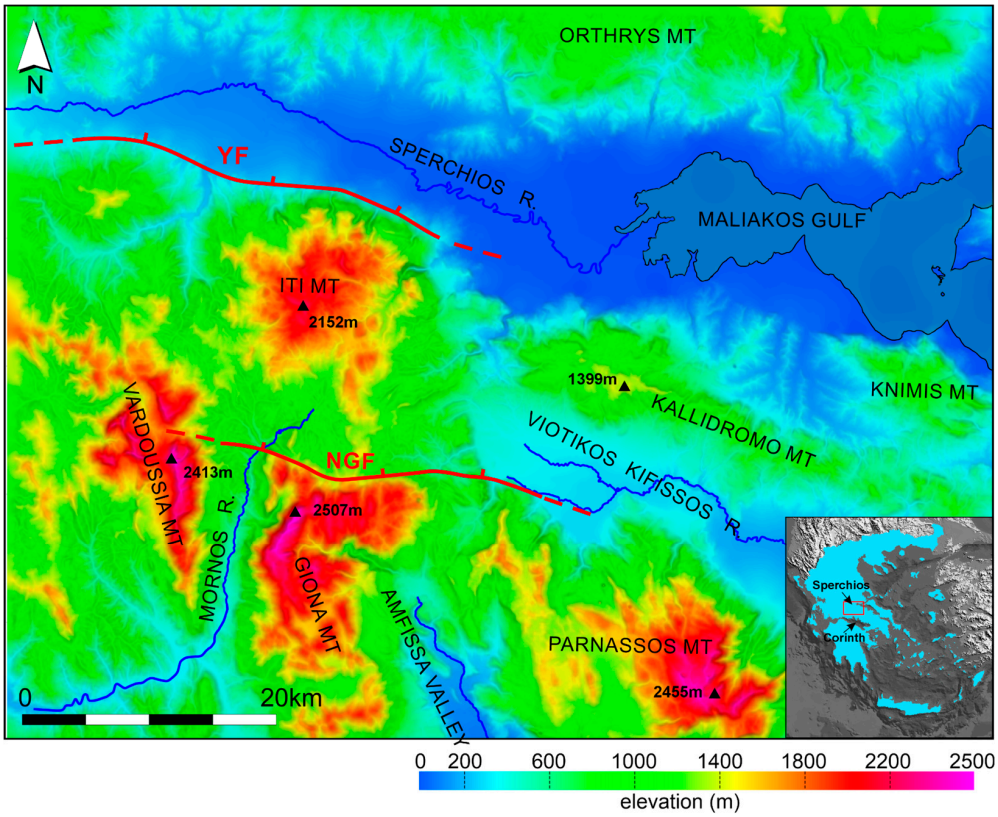

Figure 1. Morphological map of the mountainous region of central Greece between the Corinth Gulf and the Sperchios Valley/Maliakos Gulf. The northern boundary is defined by the northern slopes of Iti Mt, where the Ypati Fault (YF) creates a significant topographic difference of 2000 m, separating the mountainous area from the Sperchios Valley. To the south, the northern slopes of Giona Mt. align with the Northern Giona Fault (NGF), marking a topographic difference of 1500 m between Giona Mt and Iti Mt.

An abrupt topographic difference of more than 1500 m is observed between the Giona and Iti mountains along the northern Giona slopes, where the Northern Giona Fault (NGF) runs in an E-W direction (Figures 1 and 2). Another significant topographic difference of over 2000 m can be observed along the northern slopes of Iti Mt, toward the Sperchios River valley, where the Ypati Fault (YF) also runs E-W. These two subparallel faults have shaped the landscape, creating high mountain peaks at their northern edges on the uplifted footwalls and subsidence to the southern edges.

The prolongation of the NGF to the east-southeast aligns with the separation of the northern slopes of the Parnassos Mt from the alluvial basin of Viotikos Kifissos, where the Parnassos detachment fault (PDF—Figures 3 and 4) is observed [1,2]. To the west, the NGF reaches the Mornos river valley and likely extends further westwards bisecting the N-S Vardoussia mountain chain by lowering its northern segment for more than 1000 m.

To the north, the YF delineates the steep slopes of Iti Mt, which borders the Sperchios Valley to the south, featuring several fault scarps depicted on geological maps [3,4]. This fault is also linked to the region's geothermal activity, including the Ypati thermal springs [5]. In contrast, the NGF is less well-documented, with only small-scale fault surfaces indicated on geological maps and morphotectonic descriptions [6].

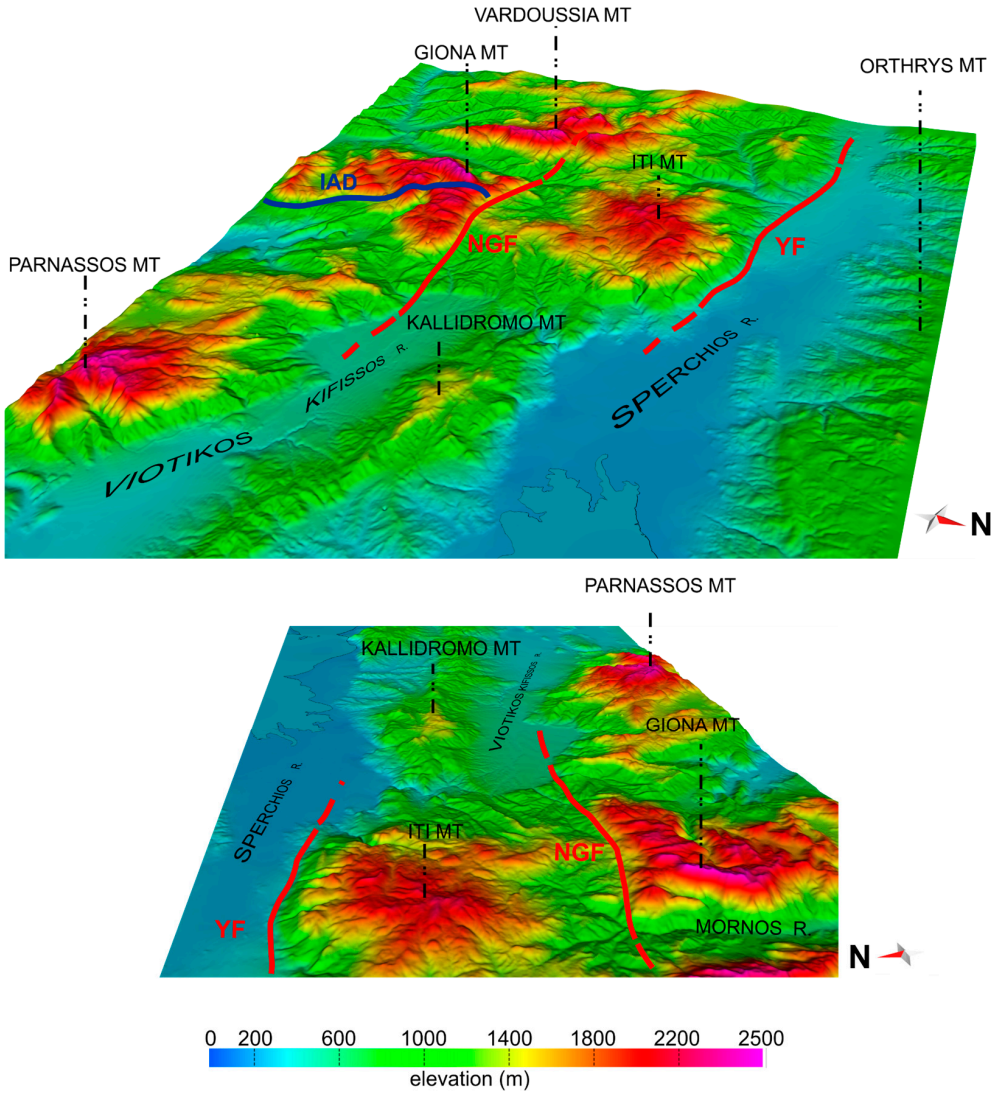

Figure 2. Three-dimensional perspective of the studied area with view from the east-northeast (**top**) and view from the west (**bottom**). In both views, the NGF and YF are indicated along the abrupt northern slopes of Giona and Iti Mts, respectively. These two subparallel faults have shaped the landscape, creating high mountain peaks at their northern edges on the uplifted footwalls and subsidence to the southern edges.

Focal mechanism solutions and earthquake data with M > 4, from the instrumental and historical catalogues of the National Observatory of Athens (NOA—http://emsc-csem.org, accessed on 30 September 2024) indicate a N-S extensional deformation in the area together with some NE-SW strike-slip events (Figure 3). GPS velocity vectors show a 20 mm/year average rate towards the SW relative to stable Africa [7,8] (Figure 3). However, the majority of the seismic events are observed in the eastern area of the Viotikos Kifissos Basin, Kallidromon and Knimis Mts, corresponding to the activation of WNW-ESE faults and only two events have occurred within the framework of the NGF (shown by the dashed rectangle in Figure 3), one with magnitude > 5.5 from historical catalogues and one > 4.5 from instrumental catalogues (see more details in the Section 5). This active deformation occurs within a broader zone that extends between the North Aegean Trough and the Kefalonia right-lateral shear zone, and is referred to as the Central Hellenic Shear Zone (CHSZ; [9]).

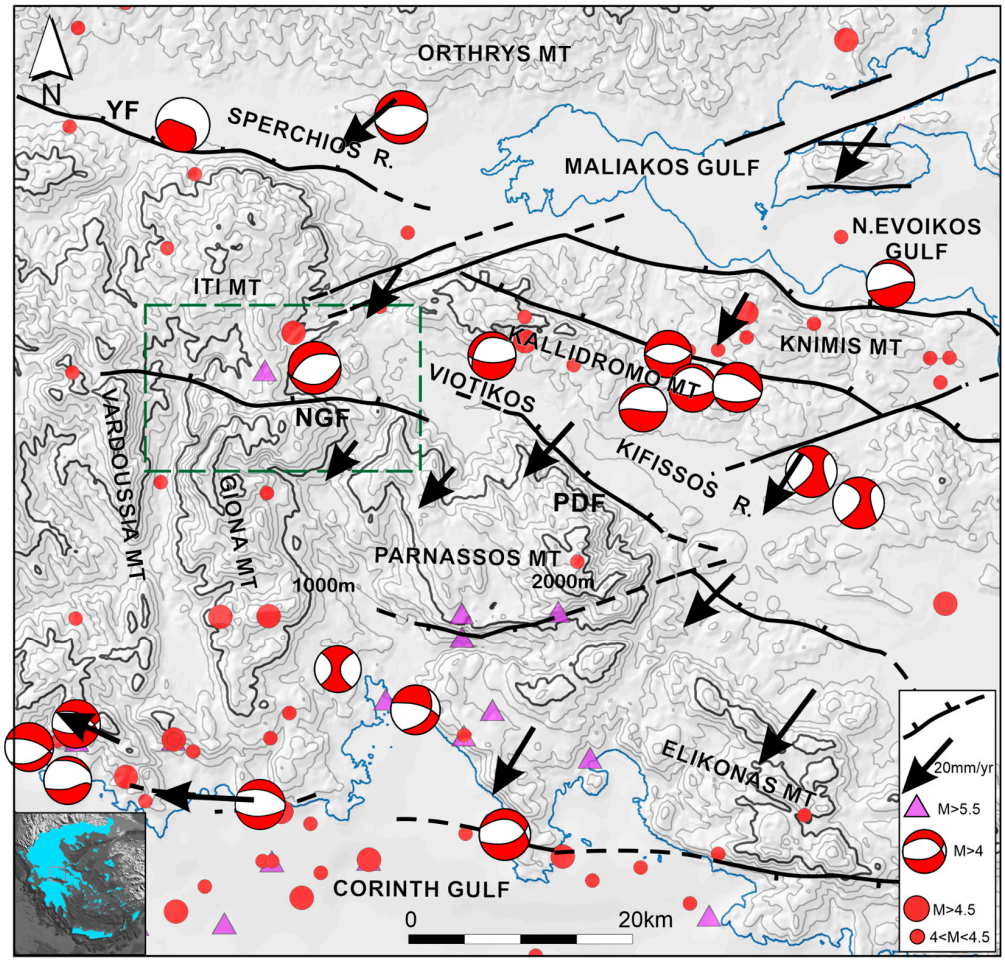

Figure 3. Map illustrating the distribution of seismic epicenters for instrumental (solid circles) and historical earthquakes (purple triangles), along with focal mechanisms for M > 4 (NOA—http://emsc-csem.org), GPS velocity vectors [7] and neotectonic faults (black lines). Central Greece's active deformation results primarily from displacements on E-W-trending faults and some NE-SW strike-slip events.

In this structural context, the detailed mapping and analysis of large morphotectonic structures, particularly those oriented perpendicular to the minimum horizontal stress axis, such as the NGF, are of major importance, since the possibility of being critically stressed is very high. Given its potential implications for the regional neotectonic framework, careful consideration of its activity is essential, as it may pose a significant and elevated seismic hazard in the area.

2. Geological Background

The geological structure of the area comprises three key components: (1) The Alpine basement rocks, consisting of multiple nappes, emplaced during the Eocene-Oligocene period, accompanied by significant thrusting and folding [10,11]. (2) Small outcrops of Oligocene-Middle Miocene molassic sediments [12] unconformably overlie the Parnassos flysch and the overlying nappes of the Beotian and Eastern Greece units [3,13]. Especially along the eastern slopes of Giona Mt the molassic sediments are part of the Itea–Amfissa basin, on the hanging wall of the Itea–Amfissa Detachment (IAD) [12] (Figure 4). (3) Late Miocene-Quaternary sediments are found within the neotectonic basins of the WNW-ESE Viotikos Kifissos and the E-W Sperchios rivers, representing post-orogenic deposits (Figure 4).

The nappes were emplaced from east to west during Eocene-Oligocene, following the deposition of flysch in each unit. The lower and more external tectonic unit is the Pindos nappe, which consists of Mesozoic sedimentary rocks such as pelagic carbonates and radiolarites [11,14–16] (Figure 4). Transitional formations with slope facies between the Pindos pelagic basin to the west and the Parnassos carbonate platform to the east occur along the Corinth coastal zone in the south, belonging to the Penteoria and the Vardoussia units [13,17–22]. The Mornos River, running N-S, separates the Vardoussia unit to the west from the Parnassos unit to the east, with the frontal thrust extending along the western slopes of Giona Mt [11].

The Parnassos unit comprises a carbonate sequence of approximately 3 km thickness of Middle Triassic–Maastrichtian age with a Paleocene-Eocene flysch on top. It is characterized by three main bauxite horizons, b1-Middle/Late Jurassic, b2-Late Jurassic/Early Cretaceous, b3-Aptian/Early Turonian [10,23]. It crops out both in the Giona and Parnassos mountain chains, extending eastward also to Elikonas Mt [24–27] (Figure 4). It also forms the basal unit in Iti Mt, north of Giona Mt, up to the Sperchios River [28]. On the northeastern slopes of Iti, Parnassos and Elikonas mountains, outcrops of the overlying Beotian unit are found [29–35]. The Beotian unit is characterized by the Late Jurassic-Early Cretaceous flysch which is followed by Late Cretaceous pelagic and slope limestones and Eocene flysch, belonging to the transitional zone between the External and the Internal Hellenides [36,37].

Tectonic klippen of the Eastern Greece unit are observed in several outcrops in Iti Mt to the north [38] and in the Kallidromo, Knimis and Orthrys Mts to the northeast [28]. The Eastern Greece unit is a synthetic Tertiary nappe comprising the Sub-Pelagonian and Maliac paleo-alpine units, overlain by the Jurassic ophiolite nappe, transgressive Late Cretaceous limestones and Paleocene-Eocene flysch [37]. Some tectonic klippen of this upper nappe are also found on Parnassos Mt [24,25], within younger NNW-trending grabens, always overlying the Beotian unit [32,33,39].

The emplacement of the nappes during the Eocene-Oligocene and the associated folding and thrusting was followed by extension during the Miocene. This extension is documented by the activation of the Middle-Late Miocene Itea-Amfissa extensional detachment (IAD in Figure 4) along the eastern slopes of Giona Mt [12] that can be traced for 30 km from the Corinth shoreline at Galaxidi to the northern crest of Giona Mt at 2000 m altitude. The basal unconformity of the shallowing-upward supra-detachment basin also follows the same southward-dipping trend and its upper members are submerged below the Itea Gulf [12,13,37].

During the Pliocene-Quaternary period, post-orogenic structures developed within the Central Hellenic Shear Zone [9] (Figure 4 inset). The post-orogenic subsidence of the nappe pile in southern Iti Mt is evident in a transverse regional geological section, where the Parnassos and overlying Beotian and Eastern Greece nappes display a southward-tilted geometry between the NGF to the south and the YF to the north (Figure 4). During this period, continental deposits accumulated in newly formed WNW-ESE neotectonic grabens along the margins of the Northern Evoikos Gulf (Figures 3 and 4; for detailed stratigraphy and geometry of the sedimentary fill of the grabens to the east, see [2] and references therein).

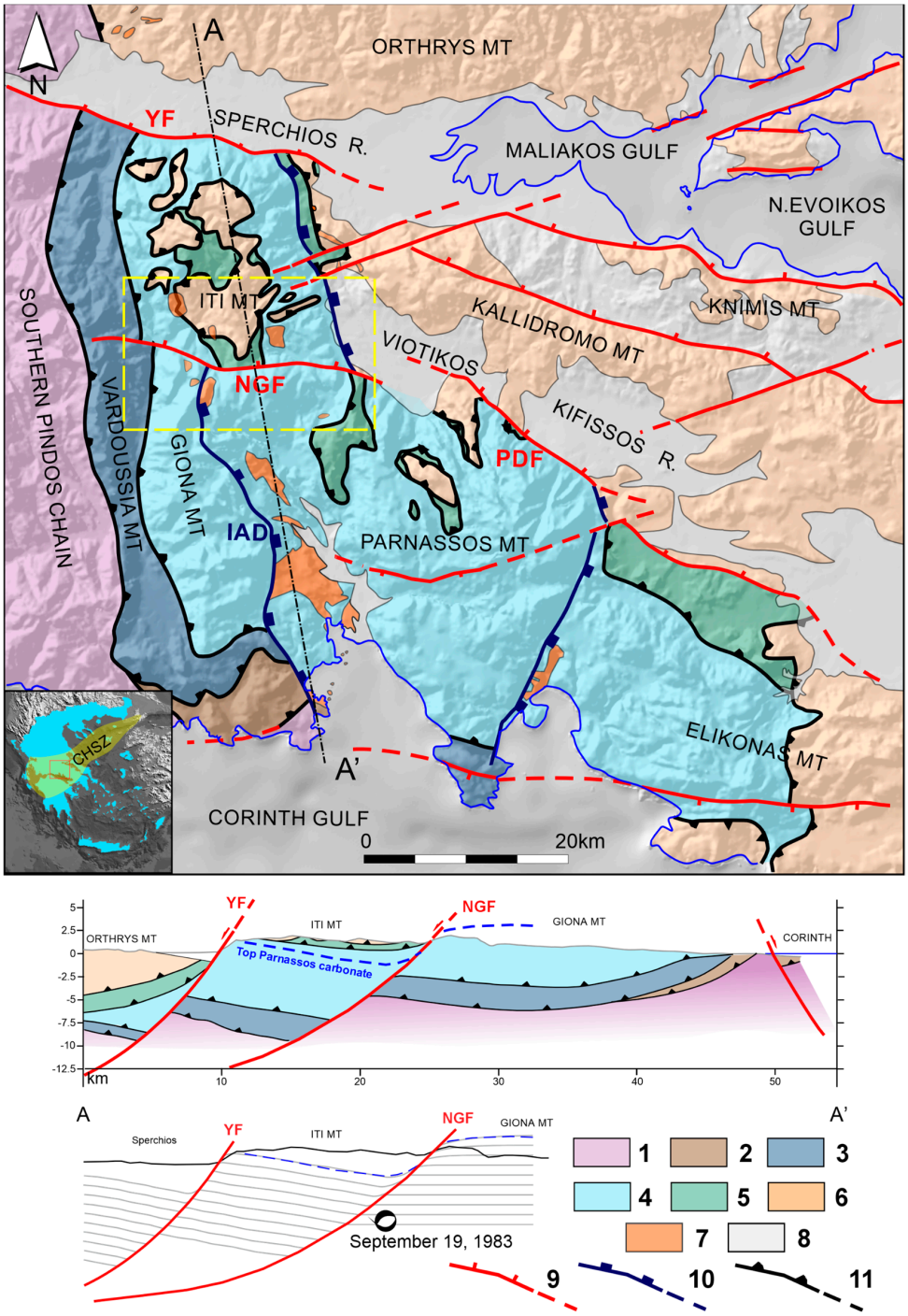

Figure 4. (**Top**) Geotectonic map of the mountainous region of central Greece between the Sperchios valley to the north and the Corinth gulf to the south. Yellow dashed rectangle shows the extent of the detailed geological map along the NGF of Figure 6. (**Middle**) NNW—SSE cross section from the Orthrys Mt to the Corinth Gulf showing the geometry of the alpine units and the major neotectonic boundaries, including the YF and the NGF. Dashed blue line indicates the top carbonate of the Parnassos unit. (**Bottom**) 2D forward model across the NGF showing the deformation of a 10 km layer-cake model with the top horizon corresponding to the pre-Pliocene tectonic framework as built in Figure 11. The Mw 5.1 19 September 1983 earthquake is plotted on the profile alongside the NGF. 1: Pindos Unit, 2: Penteoria unit, 3: Vardoussia unit, 4: Parnassos unit, 5: Beotian unit, 6: Eastern Greece unit, 7: Late Oligocene–Miocene molassic sediments, 8: Late Miocene-Quaternary sediments, 9: Neotectonic and active fault, 10: Miocene Extensional Detachment, including the Itea-Amfissa detachment (IAD) 11: major thrust fault.

3. The Northern Giona Fault Zone

The Northern Giona Fault zone is a prominent feature along the northern slopes of Giona Mt, extending for several kilometers (Figure 5). Its trace is visible in numerous outcrops along the slopes, though in certain areas it is obscured by scree and vegetation. The carbonate rocks of the footwall are characterized by intense relief and a lack of vegetation above altitudes of 1600–1800 m. The sharp topographic contrast between the Giona summits (2507, 2316, 2177 and 2063 m) and the vegetated landscape of the southern Iti is impressive. The villages of Stromi, Panourgias and Kaloskopi are situated within the subsided zone between the Giona and Iti mountains, while the villages of Mavrolithari and Pavliani lie a few km to the north, on the southern slopes of Iti Mt, at altitudes between 1000 and 1100 m (Figure 6). The village of Gravia is also located along the eastern edge of this zone, though at lower elevation, due to its intersection with the Parnassos Detachment Fault.

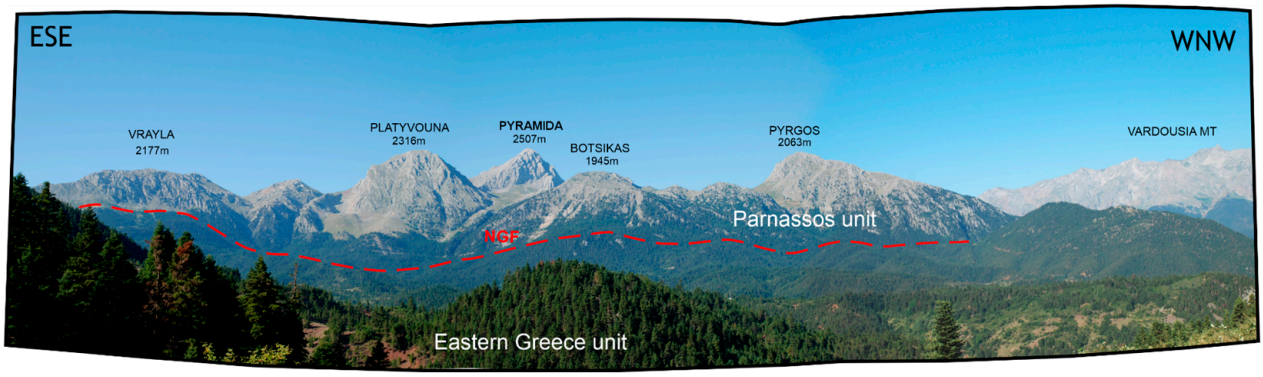

Figure 5. Panoramic view looking SSW of the NGF (red dashed line) along the northern slopes of Giona Mt. The high-elevated area of northern Giona belonging to the Parnassos unit occur in the footwall whereas the ophiolites and related sediments of the uppermost Eastern Greece unit occur in the hanging wall.

The detailed geological structure along the NGF is shown in the geological map and cross-section of the area between the northern Giona and southern Iti ranges (Figure 6). The Parnassos Unit crops out in the footwall of the NGF, with a well-exposed basal thrust to the west upon the Eocene flysch of the Vardoussia Unit along the eastern slopes of the Mornos River Valley. In the central part of the NGF, directly north of Vrayla and Lyritsa peaks, the Parnassos carbonate sequence is divided into two members; a lower member of Late Jurassic age (Js) and an upper member of Late Jurassic-Early Cretaceous age (J13-K6), separated by a bauxite horizon (b2, as described by [24]). Towards the NGF, the west-dipping carbonates of the Parnassos Unit, along with the bauxite horizon and their internal thrust faults, bend to the north, becoming parallel to the NGF (Figure 7). This pronounced change in dip and dip azimuth of the geological formations is indicative of a kilometric-scale normal drag zone that has developed in close proximity to the NGF and can be followed along the footwall for several kilometers. Bending of the west-dipping thrust faults of the Botsika and Platyvouna summits to the west and of the carbonates of the Beotian nappe to the east confirms the effect of the NGF on the pre-existing tectonic structures (Figure 6). Within this drag zone, the carbonates show missing sections, intense bed-parallel slip deformation and increased density of secondary synthetic faults.

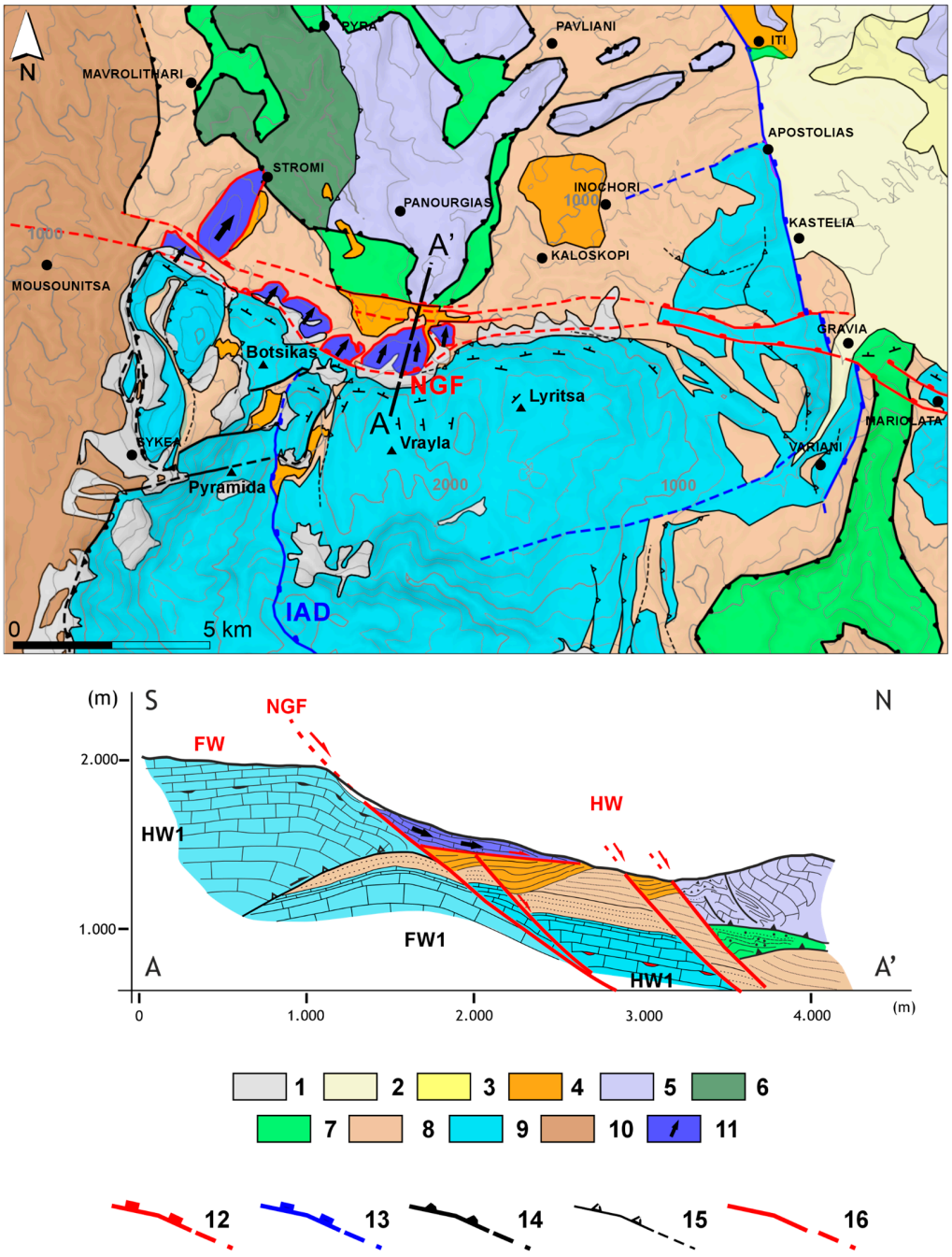

Figure 6. Geological map and cross section of the northern Giona region. 1: alluvial deposits, 2: scree deposits, 3: Neogene deposits, 4: Molassic sediments of Oligocene—Middle Miocene, 5: Triassic—Jurassic carbonates of the SubPelagonian unit, 6: Jurassic ophiolites, 7: Beotian Unit with Jurassic—Cretaceous pelagic limestones, 8: Eocene flysch of the Parnassos unit, 9: Mesozoic Carbonate platform of the Parnassos unit, with an older b2 (black) and a younger b3 (red) bauxite horizons in the cross section, 10: Eocene flysch of the Vardousssia unit, 11: Olistholites mainly of Carbonate rocks, 12: Neotectonic and active normal fault, 13: IAD, Itea-Amfissa Detachment, Miocene extensional Detachment, 14: Overthrust, 15: thrust, 16. Base of gravity slide. FW1, HW1: Imbricated tectonic units of the Parnassos nappe. FW, HW: NGF's footwall and hanging wall.

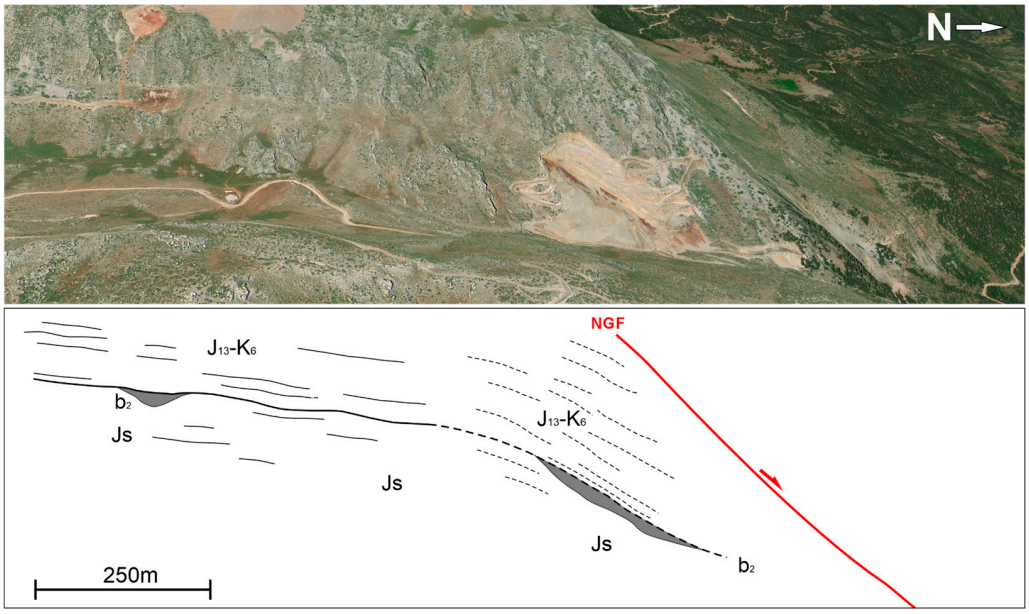

Figure 7. View to the west of the footwall at the central part of the NGF, directly east of the Vrayla peak, at 1800–2000 m altitude. The Parnassos carbonate sequence is characterized by two members in this site: a lower one of Late Jurassic age (Js) and an upper one of Late Jurassic-Early Cretaceous age (J13-K6) separated by a bauxite horizon (b2—[24]). In the sketch, solid lines indicate W-dipping strata, while dashed lines indicate N-dipping strata. This change in dip azimuth is characteristic of a kilometric scale normal drag developed near the NGF.

In the central segment of the footwall of the NGF (FW), the imbricated carbonates of the Parnassos unit consist of two tectonic units (FW1 and HW1). Displacement along the NGF, juxtaposes the flysch of the upper tectonic unit of the footwall (HW1) against the lower tectonic unit (FW1) within the hanging wall (HW) (Figure 6 geological section). However, the absence of clear lithological correlations between the eroded footwall (FW) and the hanging wall (HW), along with uncertainty regarding the throw of various synthetic faults within the fault zone, greatly complicates any attempt to accurately quantify the fault throw and total displacement of the NGF zone.

One of the most prominent outcrops of the NGF is found southwest of Kaloskopi village, along steep slopes beneath loose breccias (Figure 8). At two key locations along this tectonic contact large fault planes display well-defined grooves and striations, clearly indicating top-to-N movement. The lower site is distinguished by the contrast between the striated fault plane and the overlying loose material, comprising breccia and mixed soil. The upper site displays a 15–20 m-high fault surface that dips 35° to the north.

The NGF can be measured at several other locations along the high slopes of the mountain (Figure 9A,B) and within the bauxite mines west of Gravia (Figure 9C,D). Fault surfaces are typically planar (Figure 9B), though some segments display curvature (Figure 9D). In the central part of the fault zone, secondary faults developed on both carbonates and consolidated carbonate breccia, can be followed for several hundred meters (Figure 9A). In certain areas, characteristic cross-sections of the faults showcase their internal architecture, with well-developed damage zones that grade to thick fault cores with successive generations of cataclastic rocks (Figure 9C). The main fault, observable at high altitudes, is accompanied by secondary synthetic faults at lower altitudes. These faults have discontinuous outcrops due to the thick scree formations covering most of the slopes.

Figure 8. View from the east of the NGF. Two notable sites (**A**,**B**) where the grooved and striated fault surface is exposed and measurable, showing top-to-N movement.

The western extension of the NGF within the Mornos valley aligns with a series of E-W-trending linear ridges and steep valleys stretching from the Mornos river to the village of Athanasios Diakos. In this 3 km section the Vardoussia flysch formations are highly deformed, extensively eroded, locally covered by thick layers of soil, obscuring fault surfaces and morphological scarps. The Mornos River has no river terraces and runs directly on the eroded flysch sediments. The Mornos drainage network in the zone of the western prolongation of the NGF shows a significant change of its N-S main stream by the development of two major tributaries, one towards the east draining the northern Giona slopes in the area of Stromi village and another towards the west draining the northern Vardoussia slopes along the saddle separating the main Vardoussia Mt from its minor northern prolongation (see also Figure 12). The structure across the Vardoussia fault is similar to that of the NGF with Triassic-Jurassic limestones and cherts at the footwall and Eocene flysch at the hanging wall, usually covered by scree deposits.

Inversion of fault-slip data measured along a total number of 16 large (>100 m length) fault planes of the north Giona fault zone, following the direct stress inversion method [40] using the TectonicsFP© software [41] reveals a mean slip vector of 45°, N004°E (Figure 10). The resulting stress tensor show that the extension direction for both σ3 and T axes is N-S. This extension direction aligns with the current regional extensional orientation as corroborated by focal mechanisms solutions (Figure 3) and the calculated strain from GPS data.

South of the Gravia village, within the footwall of the NGF, lies the well-developed NNW-trending "Gerolekas Dekkengraben" [11,32,33,39,42] where the Beotian Unit tectonically overlies the Parnassos flysch (Figures 4 and 6). This graben post-dates the Late Eocene thrusting of the Beotian unit on top of the Parnassos unit and pre-dates the activity of the NGF. North of it, in the hanging wall of the NGF, a well-known NNW-SSE fault, the Kastelia–Iti fault, can be traced from the area west of Gravia to Iti village (Figure 6) and

further north up to the Dyo Vouna village [43]. This extensional fault zone shares some common characteristics with the Itea-Amfissa detachment (IAD) to the south, including intermediate to low angle dips, NNW-SSE orientation, NE- to ENE-directed extension, local reuse of older thrust faults and disruption of Oligo-Miocene molassic sequences in both the footwall and hanging wall. A notable difference from the IAD is the presence of Plio-Quaternary continental deposits in its hanging wall. Therefore, it is likely that this fault represents an older Miocene extensional structure that was later disrupted by the NGF to the south and the YF to the north.

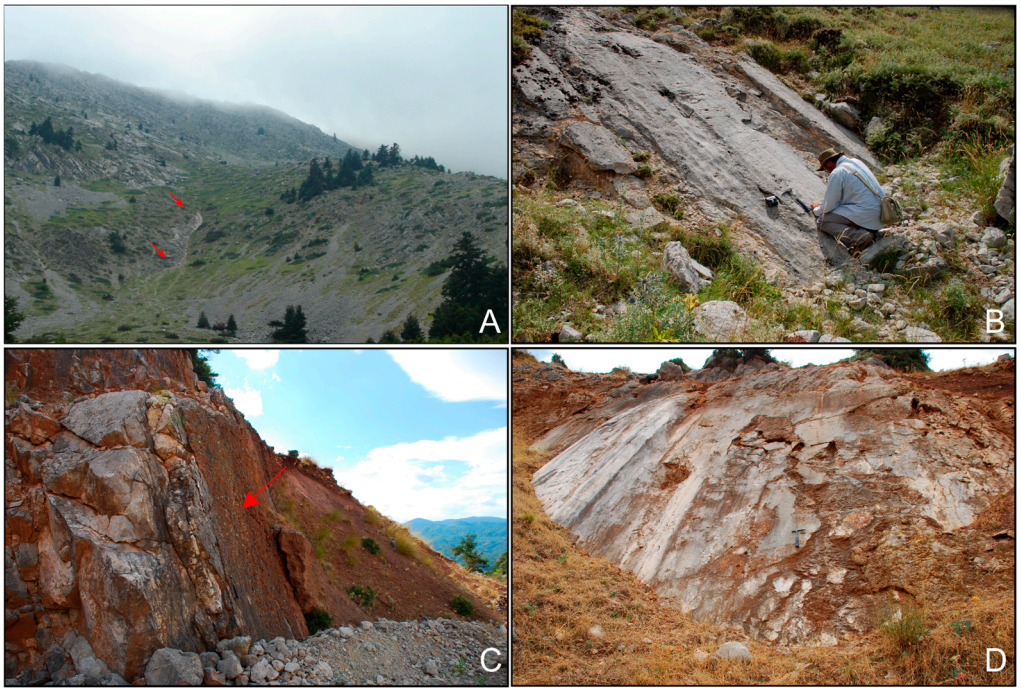

Figure 9. Outcrops of the fault surfaces along the northern Giona slopes. (**A**) Fault surface (red arrows) at the central part of the NGF. (**B**) Close view of a north-dipping fault plane along the high slopes at the western side of the NGF. (**C**) Characteristic cross-section of the fault zone in the eastern part of the NGF, showing a well-developed damage zone that grade to thick fault core (red arrow). (**D**) Curved fault surface at the eastern termination of the NGF close to the Gravia village.

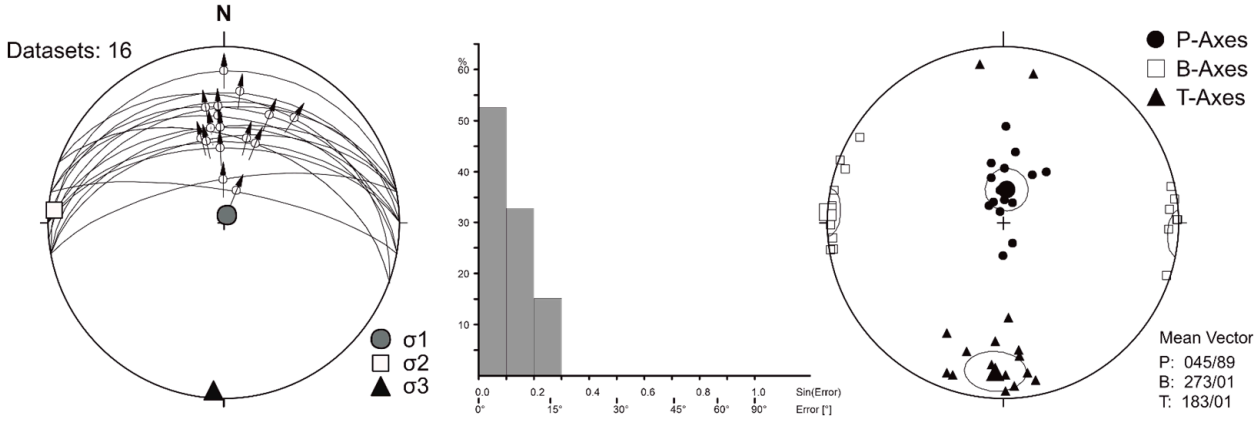

Figure 10. Fault-slip data and calculation of stress tensor with the method of direct inversion for the NGF. Lower hemisphere, equal-area stereographic projections. **Left pane** shows fault-slip data and the calculated stress axes (σ1, σ2, σ3). **Middle pane** is a fluctuation histogram of the deviation angle (angle between measured and calculated slip vectors) and stress ratio R(σ2 − σ3)/(σ1 − σ3). **Right pane** shows the P–T axes.

Another significant NNW-trending structure, the IAD, is also disrupted by the east-west NGF and cannot be traced in the hanging wall to the north (Figures 4 and 6). The Miocene molassic sediments cropping out at the northern, high-elevated zone of Giona Mt at altitudes of 1800–2100 m at the base of the Platyvouna peak (2350 m) [13], are subsided by 900–1000 m in the hanging wall, in areas east and south of Kaloskopi and Panourgias villages. The molassic sediments cropping out directly east of the Pyramida summit, unconformably cover the lower member of the Parnassos flysch, comprising red Paleocene pelites, whereas the molassic sediments on the hanging wall cover either the upper member of the thick pelitic-sandstone flysch of the Parnassos unit or the allochthonous units of Iti [13]. These relationships indicate that the flysch of the Parnassos unit and the allochthonous unit on top of it, was already eroded prior to the sedimentation of the Miocene molassic sequences. Therefore, the NGF post-dates the sedimentation of the Miocene molasse.

Although the NGF generally exhibits an E-W orientation, it is segmented. This is evidenced by changes in the orientation of the fault zone along its strike, particularly where it intersects with the older NNW-trending structures (Figure 6). In the eastern sector, near Gravia village, the NGF has a WNW-ESE orientation, changing to E-W as it intersects with the NNW-trending Kastelia-Iti fault. In the central sector, which is approximately 9 km long, the fault maintains an E-W orientation. However, east of the Botsika summit, where it merges with the IAD, the orientation shifts again from E-W to WNW-ESE. These observations indicate that the older tectonic framework plays a significant role in the linkage, segmentation and geometry of the younger NGF.

The Beotian and Eastern Greece units crop out in the hanging wall of the NGF along the southern parts of Iti Mt [38]. Jurassic ophiolites are exposed around Stromi village, and Jurassic-Cretaceous pelagic and slope sequences of the Beotian Unit are found near Kaloskopi village. These sequences are tectonically overlain by the Triassic-Jurassic sedimentary units of the Sub-Pelagonian and Maliac units within the Eastern Greece synthetic nappe, which cover most of the high Iti plateau. Both nappes rest atop the underlying Eocene Parnassos flysch in Pavliani village and various areas within the NGF hanging wall to the west. In the direct hanging wall of the NGF, numerous slide blocks of neritic limestones, derived from the uplifted footwall, represent small-scale gravity glides above flysch and molasse. These small-scale gravity nappes preserve well-developed brecciated bases (friction carpets), representing the direct fracture reservoirs for several karst springs [44].

4. Forward Modelling

Kinematic forward models are commonly used in structural geology to investigate subsurface geometries, particularly in complex tectonic settings that lack datable formations and the correlation of geological units across fault zones is generally uncertain. The workflow of a 2D kinematic forward model begins with a reference profile representing the present-day deformed state of the geological section. In our case, this reference was the regional profile illustrated in Figure 4. Along this profile, the southward-tilted geometry of both Parnassos carbonate sequence and the allochthonous nappe pile of the Iti Mt suggests gradual back-tilting of the Iti neotectonic fault block due to NGF activity.

To construct the geometry of the NGF at depth, we used this asymmetry and the mean dip of the NGF and performed slip-line analysis [45]. This analysis resulted in a northward-dipping listric geometry for the NGF (Figure 11). Based on the modeled listric fault, we next analyzed the large-scale normal drag in the NGF's footwall. Such drag across faults usually indicate heterogeneous stress and are typically linked to the development of extensional fault-propagation folds in the initial stage of their evolution. In the NGF, this fold is evident in the competent carbonate rocks of the footwall and, to a lesser extent, in the flysch of the hanging wall. The fold has been disrupted later by the upward propagation of the NGF during its maturation and progressive linkage.

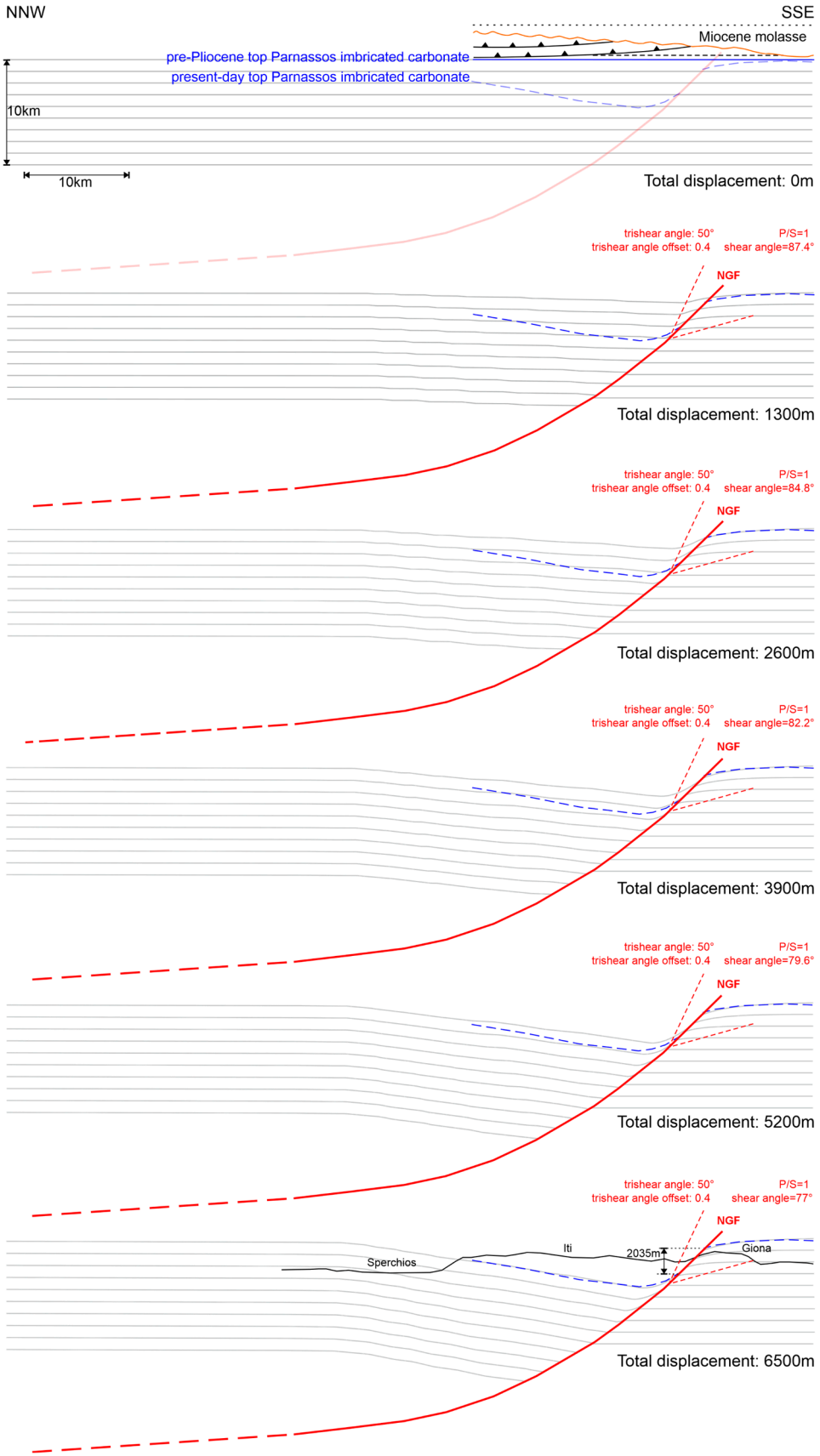

Figure 11. Construction of a 10 km-layer cake model illustrating a five-stage progressive deformation of the NGF footwall and hanging wall through the application of a trishear kinematic model with

increasing displacements of 1300 m, 2600 m, 3900 m, 5200 & 6500 m. Details of the trishear model are provided within text. The top layer represents the regional pre-tectonic level, corresponding to the pre-Pliocene deformed state, which includes early orogenic Late Eocene thrust faults (solid lines with triangles) overlying the Parnassos flysch. The Parnassos flysch comprises two members: the lower red pelites and the upper pelitic-sandstone, separated by a dashed line. Unconformably overlying these units are late-orogenic Miocene molasse deposits (wavy brown line) within the Iti and northern Giona fault blocks. The northward-dipping listric geometry of the NGF at depth is based on slip-line analysis [45].

In order to capture the complex interaction between fault propagation and related folding providing a more accurate representation of the fault-related deformation, we applied a kinematic trishear model [46–49] using MOVE©2023.1 software. Trishear algorithms generally simulate the deformation within a triangular zone ahead of the propagating fault tip, where the fold's geometry is shaped by several key parameters. These include: (i) the fault's listric shape, (ii) the trishear apical angle, (iii) the trishear angle offset and (iv) the propagation-to-slip ratio.

For the undeformed, initial state, we constructed an arbitrary layer-cake stratigraphy with 10 layers, each 1000 m thick (Figure 11). The top layer represents the regional pre-tectonic level, which, in this case, corresponds to the pre-Pliocene deformed state. The pre-Pliocene state is characterized by the older tectonic framework, which includes the early orogenic Late Eocene thrust faults and the unconformable late-orogenic Miocene molassic sedimentary sequences. In our modeling, we treated the NGF footwall as a fixed (stable) reference system and the hanging wall as the moving entity, although in reality, both may have been affected by differential uplift during the Plio-Quaternary period.

Using an iterative, trial-and-error approach, we constructed a trishear zone with a constant trishear angle of 50°, an asymmetrical zone with a trishear angle offset of 0.4, a propagation-to-slip ratio of 1 and a synthetic 77° shear angle. Through a five-stage kinematic evolution we calculated a total displacement of 6500 m and a resulting throw of 2035 m (Figure 11).

5. Discussion

The NGF has an observable length of approximately 14 km along the northern slopes of Giona Mt, extending up to 20 km between the Mornos river in the west and Gravia village in the east (Figure 6). There is potential for an additional 5 km extension westward to the Vardoussia saddle, which separates the central peak of Vardoussia from its northern segment, increasing the total length to around 25 km (Figure 1). Documenting the westward extension of the NGF is difficult because the flysch outcrops of the Parnassos and Vardoussia units do not offer measurable fault surfaces. To the east, the complexity increases as the fault zone extends beyond Gravia village, where a tectonic shift in orientation occurs along the Viotikos Kifissos. Here, the E-W-trending NGF converges with the NW-trending Parnassos detachment. Along its strike, the NGF shows changes in orientation, particularly where it intersects with older NNW-trending structures, indicating segmentation, with the central segment being approximately 9 km long. Using the inferred total (25 km) and observed length of the NGF (14 km), as well as the length of its largest segment (9 km), and applying empirical equations [50], a simple deterministic estimation of the earthquake magnitudes is as follows: a magnitude of 6.2 for a rupture of the largest segment (9 km), 6.4 for a rupture of the entire mapped fault zone (14 km) and 6.7 for the probable total length (25 km).

Considering the NGF's orientation and cross-cutting relationships with the older NNW-trending (early- and late-) orogenic structures, its activation age is post-Miocene, but there are no dateable sedimentary formations in the direct hanging wall to constrain the age in more detail, except for Quaternary scree deposits. Despite this, several features suggest a prolonged history of brittle deformation; the estimated large throw of approx. 2000 m, the presence of a thick cataclastic zone with successive layers of compact cataclasites and gradually thickening breccia that transitions into looser material (Figure 9), all indicate

extensive tectonic activity over a significant period. Moreover, the large-scale drag fold observed parallel to the fault plane immediately south of the NGF (Figure 7) suggests a rupture depth deep enough to bend the competent carbonate sequence. The observed segments of the NGF at higher elevations, between 1600 and 2000 m, likely represent deeper parts of the fault plane, possibly during its early stages in the Late Pliocene (?) or Early Pleistocene, which have been uplifted to their current position.

Earthquake catalogs for this area indicate an absence of large destructive earthquakes during the instrumental period, with only small events recorded (Figure 3). According to the historical seismicity catalog of Greece [51], no significant earthquakes have occurred in the area since at least 600 BC. However, other authors [52] reported a strong earthquake in Fokis, between the villages of Mavrolithari and Gravia, that occurred on 14 July 1852, with a magnitude of 6.1 (Figures 3 and 12). This event caused casualties in many small villages, and herds of sheep and goats were killed by rockfalls. The damage extended along the hanging wall of the Northern Giona Fault (NGF) over an approximately 20 km stretch, indicating activation of the entire fault from the Mornos River in the west to the Viotikos Kifissos basin in the east. The magnitude of this event closely aligns with the expected magnitude from a rupture of the largest segment (9 km) of the NGF, as previously deterministically estimated, though this assessment is based on macroscopic observations of seismic intensity prior to the instrumental period.

On 19 September 1983, an earthquake with a magnitude of M_L 4.6 [53] (or Mw 5.1 based on [54]) was recorded south of the Pavliani area (Figure 12). The focal mechanism indicated a normal fault striking WSW-ENE, with subsequent microseismic activity observed across the northern slopes of Giona Mt. This activity extended westward into the Mornos Valley, reaching the eastern slopes of Vardoussia Mt. The geometry of the microseismic extension likely corresponds to secondary fault planes on both the footwall and hanging wall of the NGF (Figure 12). Re-activation of older 3–4 km long ENE-WSW-trending fault planes located north of the Pyramida summit and near the village of Sykea (Figure 12 and geological map of Figure 6) may have caused the southward deviation of the microseismic activity at the western edge of the NGF in the ENE-WSW direction instead of the E-W main trend of the NGF along its central and eastern segments.

Our data from the study of the NGF necessitate a re-evaluation of the area's seismic hazard, considering the potential future activation of the NGF and its secondary effects, such as landslides and rockfalls. Especially, the northern slopes of Giona Mt that are covered with thick deposits of scree and unconsolidated material with northward-sliding olistholites (Figure 6), highlights an unstable zone, with a prolonged history of mass-wasting processes coupled with NGF seismic activity throughout the Plio-Pleistocene period. The estimated 2035 m throw of the NGF suggests a few thousand significant earthquakes, each one with 0.5–1.0 m of throw over the past 3–4 million years. The lack of major cities in the region since ancient times does not offer supplementary information on past earthquakes from the regional literature or from monastery records. Consequently, seismic events associated with the activation of the NGF in recent historical periods may have gone unrecorded.

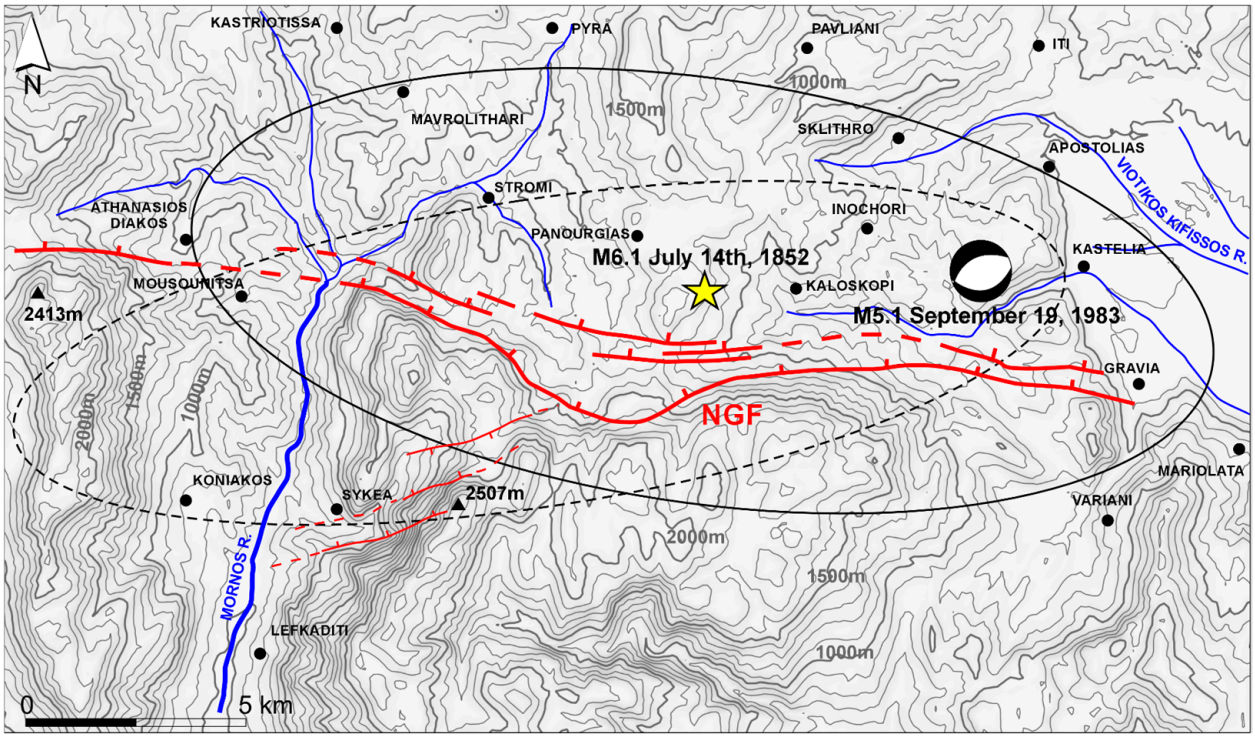

Figure 12. Map showing the spatial distribution of seismic intensity recorded by various catastrophic phenomena associated with the two significant earthquakes in the region. The solid ellipse represents the macroseismic intensities from the 14 July 1852 earthquake, which had a magnitude of 6.1 (yellow star). The dashed ellipse outlines the area affected by the microseismicity (magnitudes between 2.0 and 4.2) that followed the 19 September 1983, earthquake, which had a magnitude of 5.1 and a fault plane solution of an ENE-WSW normal fault.

6. Conclusions

In this paper, we carried-out detailed mapping of the E-W-trending, north-dipping NGF, which forms the steep northern slopes of Giona Mt, and has created a significant morphological discontinuity of nearly 1500 m (Figures 1, 2, 5 and 6). The NGF has an observable length of approximately 14 km, but may continue westward into the flysch zone between the Giona and Vardoussia mountains, potentially bisecting the northern edges of Vardoussia and reaching a total length of 25 km. It is located in a tectonically active region where seismological and GPS data indicate dominant N-S extension and minor NE-SW strike-slip faulting (Figure 3). Stress inversion of fault-slip data on the intermediate-to high-angle grooved and striated fault planes of the NGF (Figures 8 and 9) reveal a mean slip vector of 45°, N004°E, which is consistent with the regional extension (Figure 10).

Due to the absence of datable post-Alpine formations and direct lithological correlations across the footwall and hanging wall (Figure 6), we integrated stratigraphic and structural relationships between the early-orogenic alpine tectonostratigraphy and remnants of late-orogenic Miocene molassic sediments, to constrain a lower bound for the age of the NGF, that is post-Miocene. Based on the asymmetry of this older tectonostratigraphy within the NGF hanging wall, we constructed a listric fault geometry at depth using slip-line analysis (Figure 11). Additionally, with the observation of large-scale normal drag along the NGF footwall we modelled a disrupted fault-propagation fold by building a 2D kinematic trishear forward model, estimating a fault throw of approximately 2000 m and total displacement of 6500 m (Figure 11).

Given the limited seismological data available, we incorporated two significant seismic events: a historical M = 6.1 earthquake in 1852 and an instrumental M = 5.1 event in 1983 (Figure 12). The macroseismic intensity ellipse for the 1852 earthquake and the

microseismicity spatial distribution of the 1983 event align closely with the trace of the NGF, suggesting a genetic relationship with this fault, which we believe is critically stressed at depth. For the seismic potential estimation of the NGF, we adopted a deterministic approach based on the surface rupture length [51], concluding that the fault zone has the potential to produce earthquakes with magnitudes between 6.2 and 6.7.

Our study in central mainland Greece not only highlights the activity of the Northern Giona Fault, but also demonstrates that active deformation extends beyond the bounding faults of the well-documented Plio-Quaternary grabens and basins of the Northern Evoikos trough to the north and east (Figure 4), even in regions lacking datable formations. By exploring these less-studied areas, this paper aims to contribute to a more comprehensive understanding of seismic hazards and tectonic activity within the broader Central Hellenic Shear Zone of the Hellenides.

Author Contributions: Conceptualization, L.G. and D.P.; methodology, L.G. and D.P.; software, L.G.; validation, L.G. and D.P.; formal analysis, D.P.; investigation, L.G. and D.P.; resources, L.G. and D.P.; data curation, L.G. and D.P.; writing-original draft preparation, L.G. and D.P.; writing-review and editing, L.G. and D.P.; visualization, L.G.; supervision, D.P.; project administration, L.G.; funding acquisition, L.G. All authors have read and agreed to the published version of the manuscript.

Funding: This research received no external funding.

Data Availability Statement: The original contributions presented in the study are included in the article, further inquiries can be directed to the corresponding author.

Conflicts of Interest: Author Leonidas Gouliotis was employed by Energean. The remaining authors declare that the research was conducted in the absence of any commercial or financial relationships that could be construed as a potential conflict of interest.

References

1. Kranis, H.D.; Papanikolaou, D.I. Evidence for detachment faulting on the NE Parnassos mountain front (Central Greece). *Bull. Geol. Soc. Greece* **2001**, *34*, 281–287. [CrossRef]
2. Kranis, H.D. Neotectonic basin evolution in central-eastern mainland Greece. *Bull. Geol. Soc. Greece* **2007**, *40*, 360–373. [CrossRef]
3. Marinos, G.; Anastopoulos, J.; Maratos, G.; Melidonis, N.; Andronopoulos, B.; Papastamatiou, I.; Vetoulis, D.; Bornovas, J.; Christodoulou, G.; Katsikatsos, G. *Geological Map of Greece 1:50,000, Lamia Sheet*; Institute of Geology and Subsurface Research: Athens, Greece, 1967.
4. Kilias, A.; Tranos, M.; Papadimitriou, E.; Karakostas, V. The recent deformation of the Hellenic orogeny in central Greece; the Kremasta and Sperchios Fault Systems and their relationship with the adjacent large structural features. *Z. Dtsch. Geol. Ges.* **2008**, *159*, 533–577.
5. Marinos, P.; Frangopoulos, J.; Stournaras, G. La source thermomineral d' Ypati (Grece centrale). Etude hydrogeologique, hydrodynamique, geochimique et geotechnique de la source et de sa region environnante. Decouverte d' un nouveau foyer thermomineral. In *Annales Geologiques des Pays Helleniques*; Laboratoire de Géologie de l'Université: Athens, Greece, 1973; Volume 25, pp. 105–214.
6. Valkaniotis, S. Correlation Between Neotectonic Structures and Seismicity in the Broader Area of Gulf of Corinth (Central Greece). Ph.D. Thesis, Department of Geology, Aristotle University of Thessaloniki, Thessaloniki, Greece, 2009.
7. Clarke, P.J.; Davies, R.R.; England, P.C.; Parsons, B.; Billiris, H.; Paradissis, D.; Veis, G.; Cross, P.A.; Denys, P.H.; Ashkenazi, V.; et al. Crustal strain in central Greece from repeated GPS measurements in the interval 1989–1997. *Geophys. J. Int.* **1998**, *135*, 195–214. [CrossRef]
8. McClusky, S.; Balassanian, S.; Barka, A.; Demir, C.; Ergintav, S.; Georgiev, I.; Gurkan, O.; Hamburger, M.; Hurst, K.; Kahle, H.; et al. Global Positioning System constraints on plate kinematics and dynamics in the eastern Mediterranean and Caucasus. *J. Geophys. Res. Solid Earth* **2000**, *105*, 5695–5719. [CrossRef]
9. Papanikolaou, D.; Royden, L. Disruption of the Hellenic arc: Late Miocene extensional detachment faults and steep Pliocene-Quaternary normal faults—Or what happened at Corinth? *Tectonics* **2007**, *26*, TC5003. [CrossRef]
10. Papastamatiou, J. La geologie de la region Montagneuse du Parnasse—Kiona—Oeta. *Bull. Soc. Geol. Fr.* **1960**, *7*, 398–409. [CrossRef]
11. Célet, P. Contribution a étude géologique du Parnasse-Kiona et d'une partie des régions méridionales de la Grèce continentale. *Ann. Geol. Pays Hellen* **1962**, *7*, 1–358.
12. Papanikolaou, D.; Gouliotis, L.; Triantafyllou, M. *The Itea-Amfissa Detachment: A Pre-Corinth Rift Miocene Extensional Structure in Central Greece*; Geological Society London Special Publications: London, UK, 2009; Volume 311, pp. 293–310.

13. Gouliotis, L. The Tectonic Structure of Giona Mt and It's Hydrogeological Applications. Ph.D. Thesis, Department of Geology and Geoenvironment, National & Kapodistrian University of Athens, Athens, Greece, 2014.
14. Philippson, A. *Thessalien und Epirus. Reisen und Forschungen im Noerdlichen Griechenland*; W.H. Kühl: Berlin, Greece, 1897; 422p.
15. Renz, C. *Die Tektonik der Griechisch en Gebirge. Academy of Athens, Pragmatiae*; Verlag Nicht Ermittelbar: Stuttgart, Germany, 1940.
16. Renz, C. *Die Vorneogene Sratigraphie der Normal-Sedimentaren Formationen Griechenlands*; IGME: Athens, Greece, 1955.
17. Papastamatiou, J.; Tataris, A. Tectonique des sediments de transition de la zone de Parnassos—Ghiona a celle de Olonos—Pindos. *Bull. Geol. Soc. Greece* **1962**, *5*, 183–188.
18. Wiedenmayer, F. Sur quelques ammonites provenant d'un gisement a cephalopods a Penteoria (Grece). *Bull. Geol. Soc. Greece* **1963**, *5*, 28–40.
19. Johns, R. Mesozoic carbonate rudites, megabreccias and associated deposits from central Greece. *Sedimentology* **1978**, *25*, 561–573. [CrossRef]
20. Johns, D.R. The structure and stratigraphy of the Galaxidion region, Central Greece. In *Proceedings of the VI Colloquium on the Geology of the Aegean Region, Athens*; Institute of Geological and Mining Research: Athens, Greece, 1977; Volume 2, pp. 715–724.
21. Ardaens, R. Géologie de la Chaîne du Vardoussia; Comparaison Avec le Massif de Koziakas (Grèce Continentale). Ph.D. Thesis, Université de Lille, Villeneuve-d'Ascq, France, 1978; 234p.
22. Hofbauer, G. Stratigraphie, Fazies und Tektonik am SW-Rand des Parnass-Kiona-Gebirges (Mittelgriechenland). *Erlanger Geol. Abh.* **1985**, *112*, 11–45.
23. Carras, N. The Parnassos Carbonate Platform During the Late Jurassic—Early Cretaceous: Stratigraphy and Paleogeographic Evolution. Ph.D. Thesis, National & Kapodistrian University of Athens, Athens, Greece, 1995.
24. Papastamatiou, J.; Tataris, A.; Vetoulis, D.; Bornovas, J.; Christodoulou, G.; Katsikatsos, G. *Geological Map of Greece 1:50,000, Amfissa Sheet*; Institute of Geology and Subsurface Research: Athens, Greece, 1960.
25. Papastamatiou, I.; Vetoulis, D.; Bornovas, J.; Christodoulou, G.; Katsikatsos, G. *Geological Map of Greece 1:50,000, Amphiklia Sheet*; Institute of Geology and Subsurface Research: Athens, Greece, 1962.
26. Papastamatiou, J.; Tataris, A.; Maragoudakis, N.; Monopolis, D.; Kounis, G.; Albadakis, N.; Koukouzas, K. *Geological Map of Greece 1:50.000, Levadia Sheet*; Institute of Geology and Subsurface Research: Athens, Greece, 1971.
27. Aronis, G.; Panayiotides, G.; Monopolis, D.; Morikis, A. *Geological Map of Greece 1:50,000, Delphi Sheet*; Institute of Geology and Subsurface Research: Athens, Greece, 1964.
28. Marinos, G.; Anastopoulos, J.; Maratos, G.; Melidonis, N.; Andronopoulos, B. *Geological Map of Greece 1:50,000, Stylis Sheet*; Institute of Geology and Subsurface Research: Athens, Greece, 1963.
29. Celet, P.; Clement, B. Sur la presence d'une nouvelle unite paleogeographique el structurale en Grece continentale du Sud: L' unite du flysch beotien. *Comptes Rendus Somm. Société Géolog* **1971**, *17*, 43–47.
30. Celet, P.; Clement, B.; Ferriere, L. La zone beotienne en Grece: Implications paleogeographiques et structurales. *Eclogae Geol. Helv.* **1976**, *69*, 511–599.
31. Richter, D.; Muller, C. Die Flysch-Zonen Griechenlands, VIII Neue Vorkommen von Bootischem Flysch im nordlichen Pindos-Gebirge (Griechenland). *Z. Dtsch. Geol. Ges.* **1992**, *143*, 87–94.
32. Richter, D.; Moller, C.; Risch, H. Die Flysch-Zonen Griechenlands IX. Der bootische Oberkreide Flysch im nordlichen Parnass und im nordwestlichen Kallidromon-Gebirge (Griechenland). *Z. Dtsch. Geol. Ges.* **1994**, *145*, 274–285.
33. Richter, D.; Müller, C.; Risch, H. Die Flysch-Zonen Griechenlands XII. Das Böotikum und seine Flysche im Bereich des Iti-Parnass-Elikon-Gebirges, des nordwestlichen Kallidrohmon-Gebirges und des südwestlichen Othrys-Gebirges (Mittelgriechenland). *Neues Jahrb. Geol. Paläont. Abh.* **1996**, *201*, 367–409. [CrossRef]
34. Nirta, G.; Moratti, G.; Piccardi, L.; Montanari, D.; Catanzariti, R.; Carras, N.; Pappini, M. The Boeotian Flysch revisited: New constraints on ophiolite obduction in central Greece. *Ofioliti* **2015**, *40*, 107–123.
35. Nirta, G.; Moratti, G.; Piccardi, L.; Montanari, D.; Carras, N.; Catanzariti, R.; Chiari, M.; Marcucci, M. From obduction to continental collision: New data from Central Greece. *Geol. Mag.* **2018**, *155*, 377–421. [CrossRef]
36. Papanikolaou, D.; Sideris, C. Sur la signification des zones "ultrapindique" et "beotienne" d' apres la geologie de la region de Karditsa: L' Unite de Thessalie Occidentale. *Eclogae Geol. Helv.* **1979**, *72*, 251–261.
37. Papanikolaou, D. *The Geology of Greece. Regional Geology Reviews*; Springer Nature: Berlin/Heidelberg, Germany, 2021; 340p.
38. Wigniolle, E. Donnees nouvelles sur la geologie du massif de l'Iti (Grece continentale). *Ann. Soc. Geol. Nord* **1977**, *47*, 239–251.
39. Schwan, W. Strukturen, Kinematik und tectonische Stellung des Parnass-Ghiona-Gebirges im Helleniden-Orogen. *Z. Dtsch. Geol. Ges.* **1976**, *127*, 373–386.
40. Angelier, J.; Coguel, J. Sur une methode simple de determination des axes principaux des contraintes pur un population des failles. *Comptes Rendus L'Acad. Sci.* **1979**, *288*, 307–310.
41. Ortner, H.; Franz, R.; Peter, A. Easy handling of tectonic data: The programs TectonicVB for Mac and TectonicsFP for Windows™. *Comput. Geosci.* **2002**, *28*, 1193–1200. [CrossRef]
42. Rothenhofer, H.; Sowa, A. Eine Bootische decke bei Kaloskopi (Giona mittel Griecheland) im vergleich mit ahnlichen vorkommen im Parnass-Gebirge. In *Geological & Geophysical Research*; Papastamatiou Special Issue; IGME: Athens, Greece, 1986; pp. 419–430.
43. Chanier, F.; Ferriere, J.; Averbuch, O.; Graveleau, F.; Caroir, F.; Gaullier, V.; Watremez, L. The Main Pelagonian Detachment (MPD): Extensional reactivation of the frontal thrust of the Internal Zones of the Hellenides (Greece). *Comptes Rendus Géosci.* **2024**, *356* (Suppl. S2), 207–229. [CrossRef]

44. Gouliotis, L.; Alexopoulos, A. The discharge of the north Ghiona karst system, central Greece. In Proceedings of the 11th International Hydrogeological Congress, Athens, Greece, 4–6 October 2017; pp. 91–102.
45. Williams, G.; Vann, I. The geometry of listric normal faults and deformation in their hanging-walls. *J. Struct. Geol.* **1987**, *9*, 789–796. [CrossRef]
46. Withjack, M.O.; Olson, J.; Peterson, E. Experimental models of extensional forced folds. *AAPG Bull.* **1990**, *74*, 1038–1054.
47. Erslev, E.A. Trishear fault-propagation folding. *Geology* **1991**, *19*, 617–620. [CrossRef]
48. Hardy, S.; Ford, M. Numerical modeling of trishear fault-propagation folding and associated growth strata. *Tectonics* **1997**, *16*, 841–854. [CrossRef]
49. Allmendinger, R. Inverse and forward modelling of trishear fault-propagation folds. *Tectonics* **1998**, *17*, 640–656. [CrossRef]
50. Wells, D.; Coppersmith, K. New empirical relationships among Magnitude, rupture length, rupture width, rupture area and surface displacement. *Bull. Seismol. Soc. Am.* **1994**, *4*, 974–1002. [CrossRef]
51. Papazachos, B.C.; Papazachos, C. *The Earthquakes of Greece*; Ziti: Thessaloniki, Greece, 1989.
52. Ambraseys, N.N.; Jackson, J.A. Seismicity and strain in the Gulf of Corinth (Greece) since 1694. *J. Earthq. Eng.* **1997**, *1*, 433–474. [CrossRef]
53. Burton, P.; Melis, N.; Brooks, M. Coseismic crustal deformation on a fault zone defined by microseismicity in the Pavliani area, central Greece. *Geophys. J. Int.* **1995**, *123*, 16–40. [CrossRef]
54. Kiratzi, A.; Louvari, E. Focal mechanisms of shallow earthquakes in the Aegean Sea and the surrounding lands determined by waveform modelling: A new database. *J. Geodyn.* **2003**, *36*, 251–274. [CrossRef]